DOI: 10.1002/chem.200801154

Preferential Formation of Homochiral Helical Sandwich-Shaped Architectures through the Metal-Mediated Assembly of Tris(imidazoline) Ligands with a Set of d^3–d^{10} Transition-Metal Ions

Liwei Yan,[a] Zhen Wang,[a] Ming-Tsz Chen,[b] Ningjie Wu,[a] Jingbo Lan,[a] Xin Gao,[a] Jingsong You,*[a] Han-Mou Gau,[b] and Chi-Tien Chen*[b]

Abstract: A novel type of chiral tris-monodentate imidazolinyl ligands ((*S,S,S*)-**4** and (*R,R,R*)-**4**) has been achieved in good yields. The ligands show a strong tendency to induce the generation of the discrete sandwich-shaped M_3L_2 architectures with programmed helicity through the edge-directed complexation with a series of d^3–d^{10} transition-metal ions, while taking advantage of the steric hindrance of the bulky substituents of the imidazoline rings to avoid the formation of extended metal–organic frameworks (MOFs). In spite of different coordination geometries, monovalent metal ions (e.g. Ag^+), divalent metal ions (e.g. Pd^{2+}, Cu^{2+}, Cd^{2+}, Zn^{2+}, Co^{2+}, Mn^{2+}, and Ni^{2+}), and even trivalent metal ions (e.g. Fe^{3+} and Cr^{3+}) exhibit isostructural coordination. Installation of stereocenters fused onto the imidazoline rings results in favored handedness of the self-assemblies through the expression of molecular chirality into supramolecular helicity. In the crystal structures of $[M_3\{(S,S,S)\text{-}\mathbf{4}\}_2]$, the self-assembly has to adopt the *M* form to relax the van der Waals repulsions of the phenyl and isopropyl groups. The replacement of (*S,S,S*)-**4** with (*R,R,R*)-**4** exclusively affords the opposite helicity (*P*). These results should provide important insights for the design of chiral helical capsule-like assemblies.

Keywords: helical structures • imidazoline • sandwich complexes • self-assembly • transition metals

Introduction

Self-organization of molecules into helical, nonracemic architectures provides one of the most significant structural features relative to those represented by natural biomolecules such as double-stranded helices of nucleic acids and α-helical polypeptides.[1] In recent years, considerable effort has therefore been made to introduce helicity into artificial systems. One promising approach is to utilize coordination chemistry to direct the assembly of small-component molecules into aesthetically appealing helical architectures.[2,3] Despite significant progress, the creation of nonracemic helicity of assemblies continues to be a challenging and fascinating field of research.[4] One of the key issues in this area is how to control the expression of helicity from predesigned organic and inorganic building blocks and to prevent helix racemization.

The self-assembly through metal–ligand-directed interaction to provide discrete monodispersed and specific structures has received a great deal of attention due to potential applications in selective ionophores,[5] chiral memory[6] and amplification,[7] and molecular capsulation.[8] In particular, multi-monodentate nitrogen-containing heterocyclic rings with arene cores have recently been of increasing interest in the design and construction of a variety of sandwich-like topologies.[9] Among these discrete architectures, however, there are only a few examples based on helical structures, and in most cases the helical assemblies feature the racemic mixture of right- and left-handed forms.

Recent studies of the coordination interaction of 1,3,5-tris(1-imidazolyl)benzene (**1**) with transition metals have re-

---

[a] L. Yan, Z. Wang, N. Wu, Dr. J. Lan, X. Gao, Prof. Dr. J. You
Key Laboratory of Green Chemistry and Technology of
Ministry of Education, College of Chemistry,
and State Key Laboratory of Biotherapy, West China Medical School
Sichuan University, 29 Wangjiang Road, Chengdu 610064 (China)
Fax: (+86) 28-8541-2203
E-mail: jsyou@scu.edu.cn

[b] M.-T. Chen, Prof. Dr. H.-M. Gau, Prof. Dr. C.-T. Chen
Department of Chemistry, National Chung Hsing University
Taichung 402 (Taiwan)
E-mail: ctchen@mail.nchu.edu.tw

Supporting information for this article is available on the WWW under http://dx.doi.org/10.1002/chem.200801154.

vealed the preferential formation of a range of extended metal–organic frameworks (MOFs) rather than discrete architectures (Scheme 1).[10] In sharp contrast, the self-assembly of disk-shaped tris-monodentate ligands **2**[9a] or **3**[9b,f,h,i] with appropriate metal ions has resulted in the generation of helical sandwich-shaped complexes. Three methyl or *p*-tolyl groups were speculated to force the neighboring N-containing heterocyclic rings away from the plane of the central aromatic ring so that metal ions could be arrayed on the disk plane to form the M_3L_2 sandwich. However, these crystals were obtained as a racemate of the *M* and *P* isomers.[9b,f]

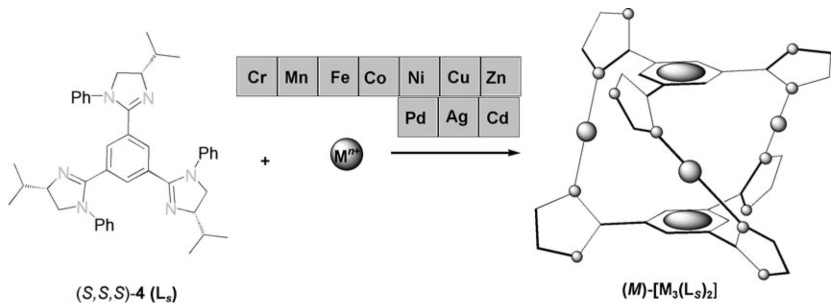

Figure 1. Schematic representation of the formation of the sandwich-shaped (*M*)-[$M_3(L_S)_2$] complexes from (*S*,*S*,*S*)-**4** and a series of different d^3–d^{10} transition-metal ions.

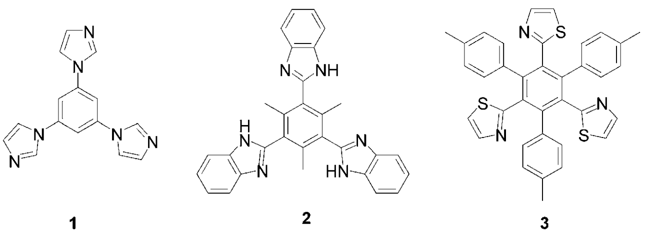

Scheme 1. Disk-shaped C_3-symmetric tris-monodentate ligands.

It is reasonable to assume that installation of stereocenters fused onto the N-containing heterocyclic rings of the disk-shaped tris-monodentate ligands should not only force the generation of sandwich-shaped M_3L_2 architectures through the edge-directed complexation of the metal ions with three ditopic tectons[11] while taking advantage of the steric hindrance of the substituents to avoid the formation of extended three-dimensional networks, but also lead to favored handedness of the self-assemblies through the expression of molecular chirality into supramolecular helicity. Imidazolines are ubiquitously biochemical, biological, and medicinal structures and function as important synthetic intermediates and auxiliaries.[12] However, to date, the use of metal-mediated assembly of imidazolines to construct supramolecular architectures is scarce. Quite recently, we described a new addition to the rational design of sterically and electronically easily tunable chiral bis(imidazoline) ligands and further demonstrated their application for highly enantioselective parent Henry reactions.[13] Herein we present a novel type of chiral tris-monodentate imidazolinyl ligands ((*S*,*S*,*S*)-**4** and (*R*,*R*,*R*)-**4**) that favor the formation of sandwich-shaped M_3L_2 architectures with predetermined chiral helicity (Figure 1). More interestingly, the self-assembly protocols exhibit isostructural coordination with a set of d^3–d^{10} transition-metal ions in spite of different coordination geometries.[8g]

Results and Discussion

Synthesis of ligands: The tris(imidazoline)benzene (*S*,*S*,*S*)-**4** was prepared according to our previously described route in excellent yield (89%).[13] The synthesis is a straightforward process, starting from the tris-amido alcohol (*S*,*S*,*S*)-**6**, which was easily prepared from readily available (*S*)-valinol and benzene-1,3,5-tricarbonyl trichloride **5**. Treatment of (*S*,*S*,*S*)-**6** with $SOCl_2$ afforded chloroethyl imidoyl chloride (*S*,*S*,*S*)-**7**, followed by chloride displacement with aniline (Scheme 2). Starting from (*R*)-valinol, the ligand (*R*,*R*,*R*)-**4** was prepared by following the same procedure as described above for (*S*,*S*,*S*)-**4**. In addition, there were no atropisomers of the ligand observed. We rationalized that it might be attributed to the rather high rotation barrier along the C_{aryl}–$C_{imidazoline}$ axis due to the steric buttressing effects by the phenyl and isopropyl groups of the imidazoline rings.

Single crystals of (*S*,*S*,*S*)-**4** suitable for X-ray analysis were obtained by recrystallization from ethyl acetate (EtOAc). The structure revealed that the three N1 atoms of each imidazoline ring in (*S*,*S*,*S*)-**4** are the coordinate sites and are on the same side of the central benzene plane (Figure 2). As expected, each imidazoline ring is out of the plane of the central aromatic ring as a result of the steric interaction that stems from the phenyl and isopropyl groups of the imidazoline rings. The dihedral angles between the three imidazoline rings and the central benzene ring are about 38°. As a consequence, such ligands should show a strong tendency to form dimeric sandwich-shaped architectures with programmed *M* or *P* helicity through the coordination of a metal ion with two N1 atoms from the different ligands. The metal ions would then be arranged on the disk plane with metal–metal distances of several angstroms.

Formation of trinuclear [$M_3(L_S)_2$] complexes: In this study, the solution behavior of (*S*,*S*,*S*)-**4** with $AgNO_3$ was initially investigated. The ^1H NMR spectrum of a mixture of (*S*,*S*,*S*)-**4** and $AgNO_3$ in a 2:3 ratio shows one set of new signals in a simple, highly symmetrical pattern, and the signals for the metal-free ligand disappear completely (Figure 3c). These results indicate the quantitative formation of a single self-assembled architecture. Surprisingly, we found that these new signals are independent of the (*S*,*S*,*S*)-**4**/$AgNO_3$ ratio. When

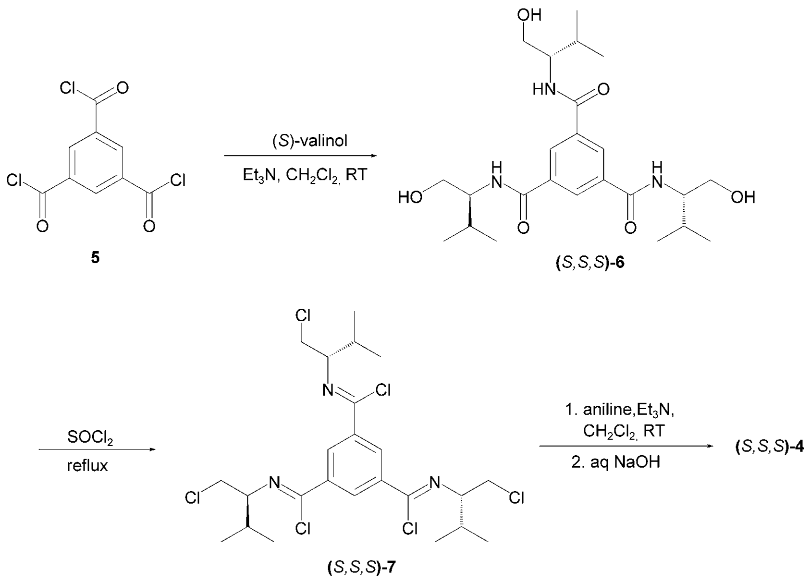

Scheme 2. Synthesis of chiral tris(imidazoline)benzene (*S,S,S*)-**4**.

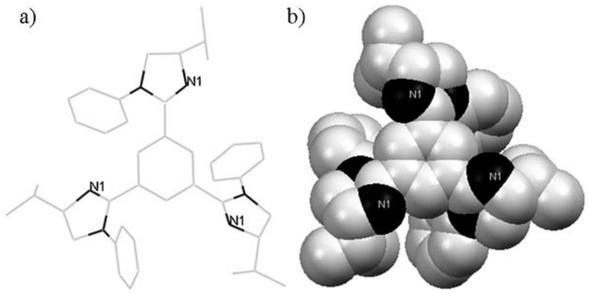

Figure 2. X-ray crystal structure of (*S,S,S*)-**4**. Color code: C (light gray), N (black), and H (omitted).

the ratio of (*S,S,S*)-**4**/$AgNO_3$ is less than 2:3, the ^1H NMR spectrum observed is similar to that for a mixture of (*S,S,S*)-**4** and $AgNO_3$ in a 2:3 ratio. As shown in Figure 3d, further addition of $AgNO_3$, up to three equivalents, did not change the ^1H NMR spectrum, although the amount of metal ion is enough for the formation of an extended metal complex. The sterically hindered interactions arising from the phenyl and isopropyl groups of the imidazoline rings appear to prevent the generation of polymeric structures. On the other hand, when the ratio of (*S,S,S*)-**4**/$AgNO_3$ is more than 2:3, the signals for the metal-free ligand clearly remains. For instance, in the presence of an equimolar amount of Ag^+ ion, two sets of signals are assigned to the self-assembled complex and the metal-free ligand (Figure 3b). A further increase in (*S,S,S*)-**4** was not capable of varying the intrinsic characteristic of the spectrum. The electrospray ionization time-of-flight (ESI-TOF) mass spectrum of a mixture of (*S,S,S*)-**4** and $AgNO_3$ in a 2:3 ratio shows a signal at *m/z* 1720.0, which is assigned to the species $[Ag_3(L_s)_2(NO_3)_2]^+$ with the loss of one NO_3^- ion. This is in good agreement with the convergence ratio of 2:3 for the (*S,S,S*)-**4**/Ag^+ observed in the ^1H NMR study. Thus, these results strongly suggest that a discrete, highly symmetrical trinuclear $[Ag_3(L_s)_2(NO_3)_3]$ complex can be exclusively formed by mixing (*S,S,S*)-**4** and $AgNO_3$ in solution.

Although the metal-mediated assembly of organic ligands to form discrete architectures has been investigated extensively, the number of metals used to maintain the shapes of the metal-assembled architectures is still limited owing to different coordination geometries. Recently, a series of 10 isostructural octahedron-shaped coordination nanocapsules were constructed from disk-shaped tris-monodentate ligands and 10 divalent d^5–d^{10} transition-metal ions by Shionoya et al.[8g] In addition to monovalent Ag^+, we further aimed to use other d^3–d^{10} transition-metal ions involving divalent and trivalent metal ions. Remarkably, monovalent metal ions (e.g. Ag^+), divalent metal ions (e.g., Pd^{2+}, Cu^{2+}, Cd^{2+}, Zn^{2+}, Co^{2+}, Mn^{2+}, and Ni^{2+}), and even trivalent metal ions (e.g., Fe^{3+} and Cr^{3+}) exhibit strong isostructural coordination with the ligand (*S,S,S*)-**4**. These self-assembled $M_3(L_s)_2$ complexes could be confirmed by NMR spectroscopy in combination with ESI-TOF mass measurements, elemental analysis, and/

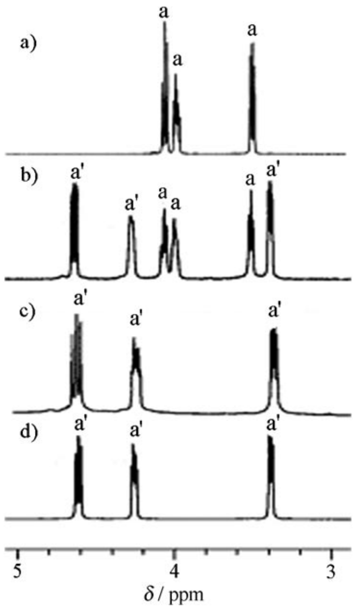

Figure 3. ^1H NMR spectra for (*S,S,S*)-**4** with $AgNO_3$ in $CDCl_3$ at 293 K (a: the metal-free ligand; a′: complex): a) the metal-free ligand (*S,S,S*)-**4**, b) (*S,S,S*)-**4**/$AgNO_3$ = 3:3, c) (*S,S,S*)-**4**/$AgNO_3$ = 2:3, and d) (*S,S,S*)-**4**/$AgNO_3$ = 1:3.

or X-ray analysis. *To the best of our knowledge, examples of self-assemblies with isostructural coordination for a broad range of metals are, hitherto, relatively rare.* The ^{1}H NMR studies indicated that the signals for the metal-free ligand (*S,S,S*)-**4** disappeared completely when 1.5 equivalents of a metal ion were added (see the Supporting Information). The ^{1}H NMR spectrum of a mixture of (*S,S,S*)-**4** and a diamagnetic divalent transition-metal ion such as Pd^{2+}, Zn^{2+}, or Cd^{2+} at a 2:3 ratio shows a similar pattern to that for the monovalent Ag^+ ion. Although paramagnetic metal complexes are known to give electronic relaxation rates large enough to prevent NMR observation,[14] in this study the paramagnetic divalent Ni^{2+} and Cu^{2+} as well as the trivalent Cr^{3+} afforded one set of relatively sharp signals, which are similar to those for diamagnetic transition-metal ions. This is probably the signature of tetrahedral coordination of the metals, which gives rise to pseudo-triply degenerated (T) electronic ground states in T_d symmetry compatible with fast electronic relaxation, thus making NMR detection possible. As shown in Figure 4b, the ^{1}H NMR spectrum for a mixture of (*S,S,S*)-**4** and $CrCl_3$ in a 2:3 ratio suggests the formation of a trinuclear $[Cr_3(L_s)_2Cl_9]$ complex. Notably, even the broadened proton signals for the paramagnetic Mn^{2+}, Co^{2+}, and Fe^{3+} ions could approximately demonstrate the quantitative formation of trinuclear $[M_3(L_s)_2]$ complexes.[8g]

The ESI-TOF spectra of the complexes of (*S,S,S*)-**4** and $PdCl_2$, $ZnCl_2{\cdot}2H_2O$, $CdCl_2{\cdot}5H_2O$, $CuCl_2{\cdot}2H_2O$, $CoCl_2{\cdot}6H_2O$, $MnCl_2{\cdot}4H_2O$, $NiCl_2{\cdot}6H_2O$, $FeCl_3{\cdot}6H_2O$, and $CrCl_3{\cdot}6H_2O$ in a 2:3 ratio show the peaks at *m/z* 1769.3, 1771.2, 1821.4, 1787.7, 1755.3, 1740.2, 1751.2, 1816.1, and 1569.4, which correspond to the species $[Pd_3(L_s)_2Cl_5]^+$, $[Zn_3(L_s)_2Cl_6{\cdot}5H_2O]$, $[Cd_3(L_s)_2Cl_6]$, $[Cu_3(L_s)_2Cl_6{\cdot}6H_2O]$, $[Co_3(L_s)_2Cl_6{\cdot}5H_2O]$, $[Mn_3(L_s)_2Cl_6.5H_2O]$, $[Ni_3(L_s)_2Cl_6{\cdot}5H_2O]$, $[Fe_3(L_s)_2Cl_9{\cdot}3H_2O]$, and $[Cr_3(L_s)_2Cl_4]^{5+}$, respectively (see the Supporting Information).

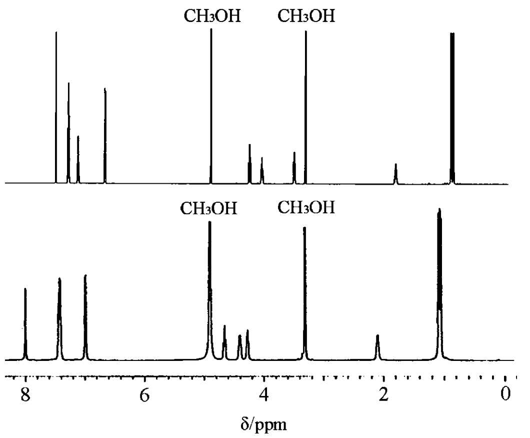

Figure 4. ^{1}H NMR spectrum for (*S,S,S*)-**4** with $CrCl_3$ in CD_3OD at 293 K: a) the metal-free ligand (*S,S,S*)-**4**, and b) (*S,S,S*)-**4**/$CrCl_3$ = 2:3.

X-ray analysis: The structures of the self-assembled complexes of (*S,S,S*)-**4** with $AgNO_3$, $PdCl_2$, and $CuCl_2{\cdot}2H_2O$ (**8**–**10**, respectively) were determined by X-ray crystallographic analyses, which provide unambiguous evidence for the formation of the sandwich-shaped trinuclear $[Ag_3(L_s)_2(NO_3)_3]$, $[Pd_3(L_s)_2Cl_6]$, and $[Cu_3(L_s)_2Cl_6]$ architectures with *M* helicity (see Table 1 for X-ray data collection parameters). In these self-assemblies, the two chiral ligands adopt a face-to-face orientation and are joined together by three metal ions to generate the individual sandwich-shaped configuration.

For $[Ag_3(L_s)_2(NO_3)_3]$ ((*M*)-**8**), the two central phenyl rings are nearly parallel to each other with an angle of 2.54° (Figure 5), which is different from those for the $[Pd_3(L_s)_2Cl_6]$

Table 1. X-ray data collection parameters for complexes (*M*)-**8**, (*M*)-**9**, (*M*)-**10**, and (*P*)-**10**.[16]

	(*M*)-**8**	(*M*)-**9**	(*M*)-**10**	(*P*)-**10**
formula	$C_{84}H_{96}Ag_3N_{15}O_9$	$C_{84}H_{96}Cl_6Pd_3N_{12}$	$C_{84}H_{96}Cl_6Cu_3N_{12}$	$C_{84}H_{96}Cl_6Cu_3N_{12}$
Fw	1799.37	1805.64	1677.06	1677.05
color	colorless	orange	olive-drab	olive-drab
crystal system	monoclinic	trigonal	cubic	cubic
space group	*P*2(1)	*R*3(2)	*P*2(1)3	*P*2(1)3
a [Å]	18.622(16)	18.416(11)	20.974(8)	20.944(6)
b [Å]	18.604(18)	18.416(11)	20.974(8)	20.944(6)
c [Å]	30.459(3)	33.875(2)	20.974(8)	20.944(6)
α [°]	90	90	90	90
β [°]	99	90	90	90
γ [°]	90	120	90	90
V [Å^3]	10414.1(17)	9950.3(10)	9227.2(6)	9187(3)
Z	4	18	12	4
ρ_{calcd} [g cm^{-3}]	1.148	0.904	1.207	1.204
F(000)	3704	2772	3492	3444
T [K]	293(2)	293(2)	293(2)	296(2)
R_1[a] ($I > 2\delta$)	0.0541	0.0421	0.0530	0.0808
wR_2[b]	0.1189	0.1016	0.1212	0.1906
GOF	0.869	0.995	1.024	1.003
μ [mm^{-1}]	0.612	0.555	0.905	0.908
Flack parameter[17]	0.01(2)	0.01(5)	0.05(2)	−0.06(5)

[a] $R1 = \Sigma(||F_o| - |F_c||)/\Sigma|F_o|$. [b] $wR2 = [\Sigma(w(F_o^2 - F_c^2)^2)/\Sigma(F_o^2)^2]^{1/2}$.

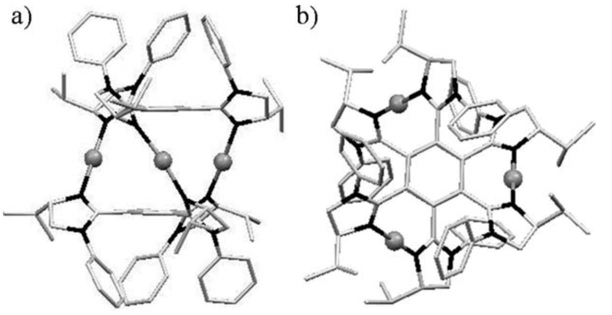

Figure 5. Crystal structure of (M)-$[Ag_3(L_s)_2(NO_3)_3]$ ((M)-**8**). a) side view, and b) top view. Color code: C (light gray), N (black), Ag (dark gray). H and NO_3^- were omitted for clarity.

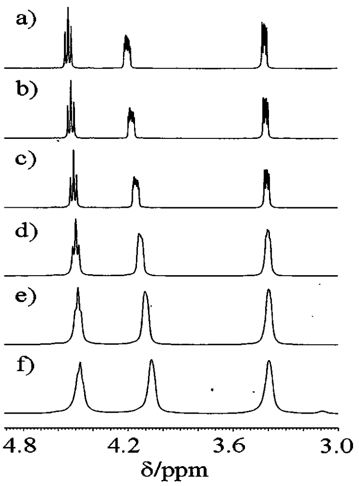

Figure 6. Variable-temperature ^1H NMR spectra of the $[Ag_3(L_s)_2(NO_3)_3]$ complex ((M)-**8**) (600 MHz, CD_2Cl_2): a) 293 K, b) 273 K, c) 253 K, d) 233 K, e) 213 K, and f) 193 K.

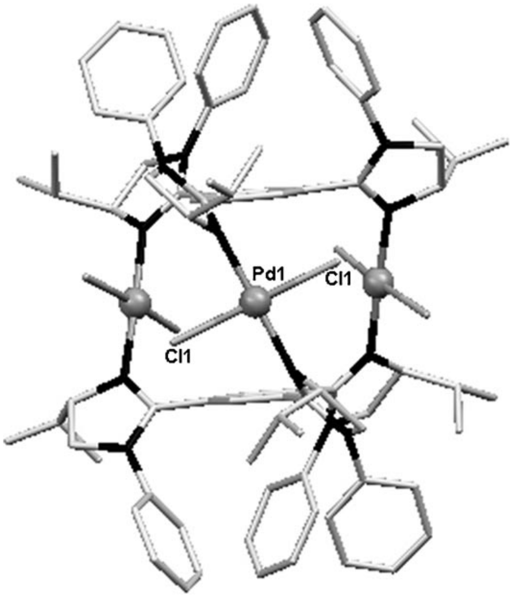

Figure 7. Crystal structure of (M)-$[Pd_3(L_s)_2Cl_6]$ ((M)-**9**). Color code: C (light gray), N (black), Pd (dark gray), and Cl (gray). All hydrogen atoms have been omitted for clarity.

and $[Cu_3(L_s)_2Cl_6]$ complexes in which the two central aromatic rings are parallel. The face-to-face distance between the two central aromatic rings is about 4.85 Å, which is longer than for aromatic π–π stacking,[9b] suggesting that the formation of the dimeric sandwich-shaped structure can apparently be attributed to metal–ligand-directed coordination. The Ag^+ ion is almost linearly coordinated with the two nitrogen atoms of the two different tripodal ligands with N-Ag-N angles of 172.31°, 174.34°, 179.13°, and the Ag−N bond lengths are between 2.09(1) and 2.12(6) Å. The intermetallic Ag−Ag distances range from 6.42 to 6.55 Å, and all nitrate ions are positioned outside the cage near the three Ag centers. The imidazoline donors are directed toward the out-of-plane of the C_3-symmetric facial ligand, and the tilting angle of about 48.30° between the central benzene and the imidazoline ring gives rise to the curvature needed for the formation of a helical structure. This capsule has to be "chirally" twisted into a left-handed form accordingly, in which the three N-Ag-N linkages are distorted from the helix axis by approximately 34°. Variable-temperature ^1H NMR measurements for the $[Ag_3(L_s)_2(NO_3)_3]$ complex showed that the signals of the imidazoline rings did not split into two sets that would arise from the mixture of the *P* and *M* isomers between 293 and 193 K, which reveals the existence of a single stable helical form of the complex in solution (Figure 6).[9b,f]

For $[Pd_3(L_s)_2Cl_6]$, the coordination environment of the divalent Pd^{2+} center is different from that of the monovalent Ag^+ ion in (M)-**8** (Figure 7). Each palladium ion is coordinated with a nearly square-planar geometry by the two Cl^- ions and the two imidazoline units. The distance between the two central aromatic rings is approximately 5.11 Å, which is the longest among the three crystals. Interestingly, the dihedral angle between the imidazoline ring and the central phenyl ring is 51.37°, which is also the largest among the three crystals. The Pd−Pd distance and the N-Pd-N angle are 6.19 Å and 177.71°, respectively. The N−Pd bond lengths are about 2.01 Å.

In contrast to $[Ag_3(L_s)_2(NO_3)_3]$ and $[Pd_3(L_s)_2Cl_6]$, each Cu^{2+} ion in $[Cu_3(L_s)_2Cl_6]$ ((M)-**10**) is tetrahedrally coordinated with two Cl^- ions and two imidazoline moieties (Figure 8a). The distance between the two central aromatic rings arranged face-to-face is about 4.09 Å, which is the shortest among the three crystals. The tilting angle between the central benzene ring and the imidazoline ring is 47.18°, which is also the smallest among the three self-assemblies. The Cu−Cu distance and the N-Cu-N angle are 6.68 Å and 157.63°, respectively. The N−Cu bond lengths range from 1.949 to 1.968 Å. In the crystal structure of trinuclear $[Cu_3(L_s)_2Cl_6]$, the self-assembly has to adopt the *M* helicity to relax the van der Waals repulsions of the phenyl and isopropyl groups on the imidazoline rings, in which all bulky substituents are away from the Cu^{2+} ions, completely preventing the formation of the *P* form. As expected, the use

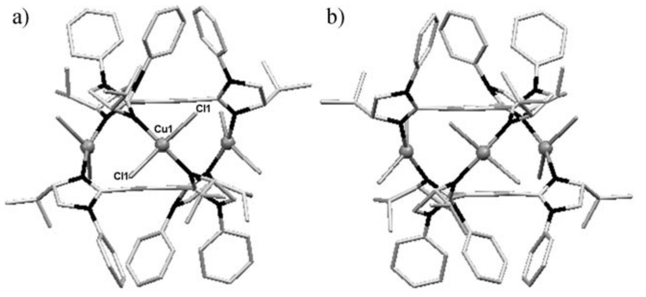

Figure 8. Comparison of crystal structures of a) (*M*)-[$Cu_3(L_S)_2Cl_6$] ((*M*)-**10**) and b) (*P*)-[$Cu_3(L_R)_2Cl_6$] ((*P*)-**10**). Color code: C (light gray), N (black), Cu (dark gray), and Cl (gray). All hydrogen atoms have been omitted for clarity.

of the ligand with *R* configuration exclusively generates the [$Cu_3(L_R)_2Cl_6$] complex ((*P*)-**10**) with right-handed *P* helicity (Figure 8b).

All attempts to obtain single crystals of the trinuclear [$Cd_3(L_S)_2Cl_6$] complex suitable for X-ray analysis were not successful. Despite the lack of X-ray crystallographic analysis, we could conclude that a single [$Cd_3(L_S)_2Cl_6$] structure was formed quantitatively in solution from the ^{1}H NMR and the ESI-TOF mass measurements. The ^{1}H NMR spectrum of a mixture of (*S,S,S*)-**4** and $CdCl_2$ (2:3) in CD_3OD at 293 K is highly symmetrical. Interestingly, the colorless crystals, which were obtained by slow vapor diffusion of diethyl ether into a DMF solution of the complex prepared from $CdCl_2\cdot 5H_2O$ and (*S,S,S*)-**4** in methanol, was confirmed to be the coordination polymer of $CdCl_2\cdot 2DMF$ by X-ray analysis (see the Supporting Information).[15] The ^{1}H NMR study illustrated that the [$Cd_3(L_S)_2$] complex is unstable in [D$_7$]DMF, affording signals identical to those of the metal-free ligand.

CD analysis: To further verify the formation of chiral helical topologies in solution, the circular dichroism (CD) spectra of (*M*)-**10** and (*P*)-**10** were studied, and the mirroring Cotton effects were observed in CH_3CN (Figure 9). The CD spectra of (*M*)-**10** showed first a positive Cotton effect followed by a negative Cotton effect at higher wavelength. The signal passes through zero around 270 nm, indicating the formation of a helical superstructure with a preferred handedness.[4] These observations clarify that the supramolecular chirality is realized by the chiral translation of the ligand.

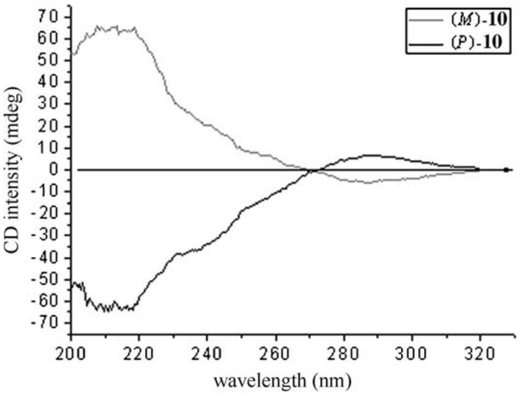

Figure 9. CD spectra of (*M*)-**10** (gray) and (*P*)-**10** (black) were observed in CH_3CN ($c = 1.5\times10^{-4}$ M).

Powder X-ray diffraction analysis: We examined the structural homogeneity of bulk powder samples of (*P*)-**10** by a comparison of experimental and simulated powder XRD (PXRD) patterns. As shown in Figure 10, the experimental pattern favorably correlates with the simulated one generated from the single-crystal X-ray diffraction data.

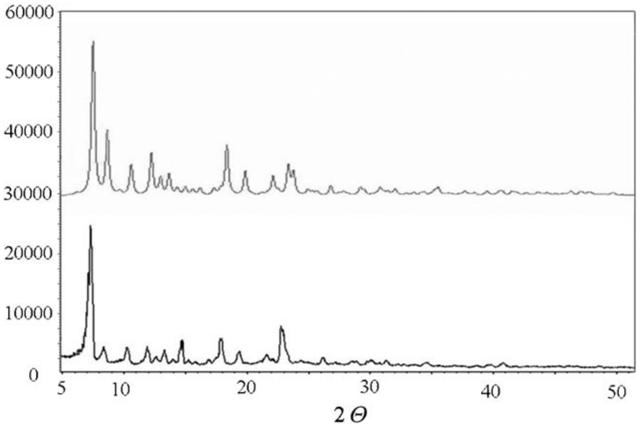

Figure 10. Comparison of powder X-ray diffraction patterns: the top and bottom patterns correspond to the simulated and experimental results, respectively.

Conclusion

In summary, this study demonstrates that a novel kind of chiral tris-monodentate imidazolinyl ligand facilitates the formation of sandwich-shaped trinuclear M_3L_2 architectures with programmed chiral helicity with a series of d^3–d^{10} transition-metal ions involving monovalent metal ions (e.g., Ag^+), divalent metal ions (e.g., Pd^{2+}, Cu^{2+}, Cd^{2+}, Zn^{2+}, Co^{2+}, Mn^{2+}, and Ni^{2+}), and trivalent metal ions (e.g., Fe^{3+} and Cr^{3+}). Installation of stereocenters fused onto the imidazoline rings leads to favored handedness of the self-assemblies through the expression of molecular chirality into supramolecular helicity. These results could give important clues to the design of chiral helical capsule-like self-assemblies. We foresee that these kinds of chiral metal complexes could impart outstanding chemical and physical properties of transition-metal ions and could be applicable in asymmetric catalysis.

Experimental Section

General remarks: ^{1}H NMR spectra were obtained on a Varian Inova-400 (400 MHz) or a Varian Inova-600 (600 MHz) spectrometer, and ^{13}C NMR spectra were recorded on a Varian Inova-400 (100 MHz) or a Varian

Inova-600 (150 MHz). Mass spectra were obtained on a BioTOF Q or a Finnigan-LCQ^{DECA} instrument. The ESI-TOF mass spectra were recorded with a Waters Q-Tof premier instrument. The high-resolution fast atom bombardment (FAB) mass spectra were obtained with a JEOL JMS-SX/SX 102 A spectrometer, and the optical rotations were determined on a WZZ-2B polarimeter. Elemental analyses were performed with a CARLO ERBA1106 instrument or a Heraeus CHN-O-RAPID instrument. Melting points were determined and are uncorrected. CD spectra were recorded on a JASCO J-500C spectropolarimeter. Unless otherwise noted, all reagents were obtained from commercial suppliers and used without further purification. Unless otherwise indicated, all syntheses and manipulations were carried out under a dry N_2 atmosphere. Anhydrous solvents were dried by using standard procedures. Benzene-1,3,5-tricarbonyl trichloride was prepared by a literature procedure.[18]

Synthesis of 1,3,5-tris((*S*)-4-isopropyl-1-phenyl-4,5-dihydro-1*H*-imidazol-2-yl)benzene ((*S,S,S*)-4): A solution of benzene-1,3,5-tricarbonyl trichloride **5** (4.8 g, 18 mmol) in CH_2Cl_2 (80 mL) was added dropwise to a stirred solution of (*S*)-valinol (5.8 g, 56 mmol) and triethylamine (9.4 mL, 68 mmol) in CH_2Cl_2 (80 mL) at 0 °C. The reaction mixture was then allowed to warm to room temperature, and stirring was continued for 12 h, followed by the addition of water (100 mL). The mixture was filtered to give the corresponding tris-amido alcohol **6** as a white solid (8.0 g, 96 %). A solution of **6** (5.0 g, 10.8 mmol) in $SOCl_2$ (20 mL) was stirred at reflux for 10 h, and volatiles were then removed under reduced pressure to afford compound **7**. CH_2Cl_2 (60 mL), Et_3N (14.0 mL, 100 mmol), and aniline (3.25 mL, 35.5 mmol) were added to the residue at 0 °C. The resulting mixture was allowed to warm to room temperature and stirred for 24 h. The solution was then washed with NaOH (10 %, 50 mL), and the aqueous layer was extracted with CH_2Cl_2 (3×60 mL). The combined organic layers were dried over $MgSO_4$ and the solvent was removed in vacuo to give a yellow solid, which could be purified by column chromatography on silica gel with elution with ethyl acetate/methanol (3:1) or by recrystallization from EtOAc to afford (*S,S,S*)-**4** as a white solid (6.1 g, 89 %). The single crystals suitable for X-ray analysis were achieved by recrystallization from EtOAc. M.p.: 232–234 °C; $[\alpha]_D^{25}=349.0$ ($c=0.5$ in CH_3OH); ^1H NMR (600 MHz, $CDCl_3$): $\delta=0.83$ (d, $J=6.6$ Hz, 9H), 0.91 (d, $J=7.2$ Hz, 9H), 1.78–1.84 (m, 3H), 3.47 (dd, $J=7.2$ Hz, 9.6 Hz, 3H), 3.94 (dd, $J=7.2$ Hz, 9.6 Hz, 3H), 3.96–3.99 (m, 3H), 6.59 (d, $J=7.8$ Hz, 6H), 6.94 (t, $J=7.2$ Hz, 3H), 7.11 (t, $J=7.2$ Hz, 6H), 7.60 (s, 3H) ppm; ^{13}C NMR (150 MHz, $CDCl_3$): $\delta=17.7$, 18.4, 32.8, 56.0, 69.9, 122.8, 123.2, 128.4, 130.1, 131.6, 142.8, 160.0 ppm; HRMS (FAB) calcd for $[C_{42}H_{48}N_6]^+$: 636.3940; found: 636.3935; elemental analysis calcd (%) for $C_{42}H_{48}N_6$: C 79.21, H 7.60, N 13.20; found: C 79.02, H 7.83, N 12.97.

Synthesis of 1,3,5-tris((*R*)-4-isopropyl-1-phenyl-4,5-dihydro-1*H*-imidazol-2-yl)benzene ((*R,R,R*)-4): Starting from (*R*)-valinol, the ligand (*R,R,R*)-**4** was prepared following the same procedure as described above for (*S,S,S*)-**4**. Yield: 90 %; m.p.: 232–234 °C; $[\alpha]_D^{25}=-349.0$ ($c=0.5$ in CH_3OH); ^1H NMR (400 MHz, $CDCl_3$): $\delta=0.85$ (d, $J=6.4$ Hz, 9H), 0.92 (d, $J=6.8$ Hz, 9H), 1.78–1.85 (m, 3H), 3.48 (dd, $J=6.8$ Hz, 10.4 Hz, 3H), 3.50 (dd, $J=6.8$ Hz, 10.4 Hz, 3H), 3.96–4.00 (m, 3H), 6.60 (d, $J=8.4$ Hz, 6H), 6.95 (t, $J=7.2$ Hz, 3H), 7.12 (t, $J=8.0$ Hz, 6H), 7.61 (s, 3H) ppm; ^{13}C NMR (100 MHz, $CDCl_3$): $\delta=17.8$, 18.5, 32.9, 56.2, 70.1, 123.0, 123.4, 128.5, 130.3, 131.6, 143.0, 160.1 ppm; HRMS (FAB) calcd for $[C_{42}H_{48}N_6]^+$: 636.3940; found: 636.3931; elemental analysis calcd (%) for $C_{42}H_{48}N_6$: C 79.21, H 7.60, N 13.20; found: C 79.13, H 7.72, N 13.01.

Synthesis of the $[Ag_3(L_S)_2(NO_3)_3]$ complex ((*M*)-8): A solution of (*S,S,S*)-**4** (50 mg, 0.0078 mmol) in methanol (2 mL) and an aqueous solution of $AgNO_3$ (1.5 equiv, 1 mL) were added to a flask wrapped with aluminum foil. The reaction mixture was stirred for 30 min and was then concentrated to dryness. Single crystals suitable for X-ray analysis were obtained by slow diffusion of diethyl ether into a solution of the corresponding compound in acetone at ambient temperatures after several days (yield 75 %). ^1H NMR (600 MHz, CD_2Cl_2): $\delta=0.80$ (d, $J=6.6$ Hz, 9H), 0.82 (d, $J=6.6$ Hz, 9H), 1.82–1.85 (m, 3H), 3.41 (dd, $J=6.0$ Hz, 10.2 Hz, 3H), 3.42 (dd, $J=6.6$ Hz, 9.6 Hz, 3H), 4.18–4.22 (m, 3H), 6.49 (d, $J=7.2$ Hz, 6H), 7.15 (t, $J=7.8$ Hz, 3H), 7.23 (t, $J=8.4$ Hz, 6H), 7.49 (s, 3H) ppm; ^{13}C NMR (150 MHz, CD_2Cl_2): $\delta=16.6$, 17.0, 33.0, 55.3, 68.8, 125.7, 126.4, 129.1, 130.6, 131.5, 139.9, 163.0 ppm; MS (ESI-TOF) (CH_3OH): *m/z*: 1551.1 $[Ag_2(L_s)_2(NO_3)]^+$, 1588.0 $[Ag_2(L_s)_2(NO_3)\cdot 2H_2O]^+$, 1632.0 $[Ag_3(L_s)_2\cdot 2H_2O]^{3+}$, 1676.0 $[Ag_3(L_s)_2(NO_3)\cdot H_2O]^{2+}$, 1721.9 $[Ag_3(L_s)_2(NO_3)_2]^+$; elemental analysis calcd (%) for $C_{84}H_{96}Ag_3N_{15}O_9$: C 56.57, H 5.43, N 11.78; found: C 55.73, H 5.27, N 11.54.

Synthesis of the $[Pd_3(L_S)_2Cl_6]$ complex ((*M*)-9): A solution of (*S,S,S*)-**4** (50 mg, 0.0078 mmol) in methanol (2 mL) was carefully layered over a solution of $PdCl_2$ (21 mg, 0.0119 mmol) in dimethyl sulfoxide (DMSO). Orange crystals were isolated after several days in 71 % yield. ^1H NMR (600 MHz, CD_2Cl_2): $\delta=0.86$ (d, $J=7.2$ Hz, 9H), 0.82 (d, $J=7.2$ Hz, 9H), 2.49–2.55 (m, 3H), 3.15 (dd, $J=6.6$ Hz, 10.2 Hz, 3H), 3.17 (dd, $J=6.6$ Hz, 9.6 Hz, 3H), 4.41–4.44 (m, 3H), 6.31 (d, $J=7.2$ Hz, 6H), 7.11–7.16 (m, 9H), 8.52 (s, 3H) ppm; ^{13}C NMR (150 MHz, CD_2Cl_2): $\delta=16.0$, 17.6, 31.3, 41.0, 69.0, 126.3, 126.5, 127.0, 129.1, 137.1, 140.5, 162.8 ppm; MS (ESI-TOF) (CH_3OH): *m/z*: 1625.5 $[Pd_3(L_s)_2Cl]^{5+}$, 1734.4 $[Pd_3(L_s)_2Cl_4]^{2+}$, 1769.4 $[Pd_3(L_s)_2Cl_5]^+$; elemental analysis calcd (%) for $C_{84}H_{96}Cl_6Pd_3N_{12}$: C 55.87, H 5.36, N 9.31; found: C 55.76, H 5.39, N 9.12.

Synthesis of the $[Cu_3(L_S)_2Cl_6]$ complex ((*M*)-10): Reaction of (*S,S,S*)-**4** (50 mg, 0.0078 mmol) with $CuCl_2\cdot 2H_2O$ (20 mg, 0.0117 mmol) gave immediate precipitation of a brown product. Olive-drab crystals of (*M*)-**10** were isolated by liquid diffusion of CH_3OH into a DMF solution of the solid after several days (61 % yield). ^1H NMR (600 MHz, CD_3OD): $\delta=0.94$ (d, $J=5.4$ Hz, 9H), 0.97(d, J=7.2 Hz, 9H), 1.94–1.94 (m, 3H), 3.91 (br, 3H), 4.28 (br, 3H), 4.47 (br, 3H), 6.80 (d, $J=5.4$ Hz, 6H), 7.28–7.37 (m, 9H), 7.67 (br, 3H) ppm; ^{13}C NMR (150 MHz, CD_3OD): $\delta=17.9$, 33.8, 57.8, 64.6, 66.8, 126.3, 128.8, 129.5, 130.9, 133.5, 139.7, 163.2 ppm; MS (ESI-TOF) (CH_3OH): *m/z*: 1605.8 $[Cu_3(L_s)_2Cl_4]^{2+}$, 1787.7 $[Cu_3(L_s)_2Cl_6\cdot 6H_2O]$; elemental analysis calcd (%) for $C_{84}H_{96}Cl_6Cu_3N_{12}$: C 60.16, H 5.77, N 10.02; found: C 59.29, H 5.55, N 9.92.

General synthetic procedure for other $[M_3(L_S)_2]$ complexes: The metal salt (0.047 mmol, 1.5 equiv) was added to a solution of (*S,S,S*)-**4** (20 mg, 0.031 mmol) in CH_3OH (3 mL). After the mixture had been stirred for 4 h at room temperature, the solvent was evaporated to afford the $[M_3(L_s)_2]$ complex, which could be purified by recrystallization.

$[Cd_3(L_S)_2Cl_6]$ complex: ^1H NMR (600 MHz, CD_3OD): $\delta=0.83$ (d, $J=6.6$ Hz, 9H), 0.89 (d, $J=6.6$ Hz, 9H), 1.94–1.97 (m, 3H), 3.62 (t, $J=7.2$ Hz, 3H), 4.13–4.14 (m, 3H), 4.34 (t, $J=10.8$ Hz, 3H), 6.73 (d, $J=8.4$ Hz, 6H), 7.16 (t, $J=7.2$ Hz, 3H), 7.30 (t, $J=8.4$ Hz, 6H), 7.63 (s, 3H) ppm; ^{13}C NMR (150 MHz, CD_3OD): $\delta=15.9$, 18.1, 31.8, 50.5, 54.6, 66.4, 124.8, 126.1, 129.0, 133.0, 139.0, 161.9 ppm; MS (ESI-TOF) (CH_3OH): *m/z*: 1633.5 $[Cd_3(L_s)_2\cdot H_2O]^{6+}$, 1663.5 $[Cd_3(L_s)_2Cl\cdot H_2O]^{5+}$, 1716.4 $[Cd_3(L_s)_2Cl_3]^{3+}$, 1733.4 $[Cd_3(L_s)_2Cl_3\cdot H_2O]^{3+}$, 1773.4 $[Cd_3(L_s)_2Cl_4\cdot H_2O]^{2+}$, 1821.4 $[Cd_3(L_s)_2Cl_6]$; elemental analysis calcd (%) for $C_{84}H_{96}Cl_6Cd_3N_{12}$: C 55.32, H 5.31, N 9.22; found: C 54.76, H 5.71, N 8.99.

$[Zn_3(L_S)_2Cl_6]$ complex: ^1H NMR (600 MHz, CD_3OD): $\delta=0.80$ (br, 18H), 2.02 (br, 3H), 3.64 (br, 3H), 4.24 (br, 3H), 4.44 (br, 3H), 6.77 (br, 6H), 7.20 (br, 3H), 7.34 (s, 6H), 7.74 (br, 3H) ppm; ^{13}C NMR (150 MHz, CD_3OD): $\delta=16.1$, 18.3, 33.0, 55.2, 67.7, 126.2, 127.8, 129.5, 130.7, 135.2, 140.5, 163.9 ppm; MS (ESI-TOF) (CH_3OH): *m/z*:1505.5 $[Zn_3(L_s)_2Cl]^{5+}$, 1647.3 $[Zn_3(L_s)_2Cl_5]^+$, 1771.2 $[Zn_3(L_s)_2Cl_6\cdot 5H_2O]$; elemental analysis calcd (%) for $C_{84}H_{96}Cl_6Zn_3N_{12}$: C 59.96, H 5.75, N 9.99; found: C 59.12, H 6.01, N 9.54.

$[Co_3(L_S)_2Cl_6]$ complex: ^1H NMR (600 MHz, CD_3OD): $\delta=2.29$ (br), 4.65 (br), 5.63 (br), 6.55 (br), 7.89 (br), 8.52 (br), 8.64 (br) ppm; MS (ESI-TOF) (CH_3OH): *m/z*: 1626.4 $[Co_3(L_s)_2Cl_5]^+$, 1755.3 $[Co_3(L_s)_2Cl_6\cdot 5H_2O]$; elemental analysis calcd (%) for $C_{84}H_{96}Cl_6Co_3N_{12}$: C 60.66, H 5.82, N 10.11; found: C 59.98, H 6.11, N 9.87.

$[Mn_3(L_S)_2Cl_6]$ complex: ^1H NMR (600 MHz, CD_3OD): $\delta=2.34$ (br, 21H), 5.57 (br, 3H), 5.79 (br, 6H), 8.15 (br, 6H), 8.63 (br, 3H), 8.76 (br, 6H), 8.96 (br, 3H) ppm; ^{13}C NMR (150 MHz, CD_3OD): $\delta=17.0$, 17.2, 32.9, 56.7, 125.0, 126.4, 129.6, 130.3, 132.0, 141.0 ppm; MS (ESI-TOF) (CH_3OH): *m/z*: 1507.6 $[Mn_3(L_s)_2Cl_2]^{4+}$, 1614.4 $[Mn_3(L_s)_2Cl_5]^+$, 1740.2 $[Mn_3(L_s)_2Cl_6\cdot 5H_2O]$; elemental analysis calcd (%) for $C_{84}H_{96}Cl_6Mn_3N_{12}$: C 61.10, H 5.86, N 10.18; found: C 60.78, H 5.98, N 9.77.

$[Ni_3(L_S)_2Cl_6]$ complex: ^1H NMR (600 MHz, CD_3OD): $\delta=0.88$–0.94 (m, 18H), 1.82 (br, 3H), 3.77 (m, 3H), 4.15–4.47 (m, 3H), 4.36–4.40 (m, 3H), 6.72–6.76 (m, 6H), 7.23–7.25 (m, 3H), 7.22–7.35 (m, 6H), 7.53–7.55 (m, 3 H) ppm; ^{13}C NMR (150 MHz, CD_3OD): $\delta = 17.8$, 17.9, 33.8, 57.4, 67.8, 125.9, 128.0, 130.7, 133.0, 140.7, 162.8 ppm; MS (ESI-TOF) (CH_3OH): m/z: 1625.3 $[Ni_3(L_s)_2Cl_5]^+$, 1751.2 $[Ni_3(Ls)_2Cl_6\cdot 5H_2O]$; elemental analysis calcd (%) for $C_{84}H_{96}Cl_6Ni_3N_{12}$: C 60.68, H 5.82, N 10.11; found: C 60.11, H 6.11, N, 9.68.

$[Cr_3(L_S)_2Cl_9]$ complex: ^{1}H NMR (600 MHz, CD_3OD): $\delta = 1.05$ (d, $J = 6.6$ Hz, 9 H), 1.08 (d, $J = 6.6$ Hz, 9 H), 2.05 (s, 3 H), 4.26 (t, $J = 8.4$ Hz, 3 H), 4.40–4.41 (m, 3 H), 4.64 (t, $J = 11.4$ Hz, 3 H), 6.98 (d, $J = 7.2$ Hz, 6 H), 7.41–7.44 (m, 9 H), 8.00 (s, 3 H) ppm; ^{13}C NMR (150 MHz, CD_3OD): $\delta = 17.8$, 17.9, 33.6, 58.6, 64.3, 126.8, 130.5, 131.3, 135.3, 136.7, 163.3 ppm; MS (ESI-TOF) (CH_3OH): m/z: 1569.4 $[Cr_3(Ls)_2Cl_4]^{5+}$; elemental analysis calcd (%) for $C_{84}H_{96}Cl_9Cr_3N_{12}$: C 57.69, H 5.53, N 9.61; found: C 57.22, H 5.71, N 9.45.

$[Fe_3(L_S)_2Cl_9]$ complex: ^{1}H NMR (600 MHz, CD_3OD): $\delta = 1.07$ (br, 18 H), 2.18 (br, 3 H), 4.32 (br, 3 H), 4.51 (br, 3 H), 4.68 (br, 3 H), 7.01 (br, 6 H), 7.42 (br, 9 H), 8.00 (br, 3 H) ppm; ^{13}C NMR (150 MHz, CD_3OD): $\delta = 19.3$, 34.9, 62.1, 65.7, 126.7, 129.4, 131.1, 132.3, 136.5, 140.7, 163.4 ppm; MS (ESI-TOF) (CH_3OH): m/z: 1617.3 $[Fe_3(L_s)_2Cl_5]^{4+}$, 1652.3 $[Fe_3(L_s)_2Cl_6]^{3+}$, 1780.1 $[Fe_3(L_s)_2Cl_9\cdot H_2O]$, 1816.1 $[Fe_3(L_s)_2Cl_9\cdot 3H_2O]$, 1853.0 $[Fe_3(L_s)_2Cl_9\cdot 5H_2O]$; elemental analysis calcd (%) for $C_{84}H_{96}Cl_9Fe_3N_{12}$: C 57.31, H 5.50, N 9.55; found: C 56.45, H 5.71, N 9.13.

Acknowledgements

This work was supported by grants from the National Natural Science Foundation of China (Nos. 20572074, 20602027 and 20772086), the Program for New Century Excellent Talents in University (NCET-04—0881), and the Outstanding Young Scientist Award of Sichuan Provinces. We thank the Centre of Testing and Analysis, Sichuan University for NMR, CD, X-ray, and XRD measurements.

---

[1] a) J. D. Watson, F. H. C. Crick, *Nature* **1953**, *171*, 737–738; b) L. Pauling, R. B. Corey, H. R. Branson, *Proc. Natl. Acad. Sci. USA* **1951**, *48*, 205–211; c) N. Sewald, H.-D. Jakubke, *Peptides: Chemistry and Biology*, Wiley-VCH: Weinheim, **2002**.

[2] a) J.-M. Lehn, *Supramolecular Chemistry: Concepts and Perspectives*, VCH: Weinheim, **1995**; b) M. Albrecht, *Angew. Chem.* **2005**, *117*, 6606–6609; *Angew. Chem. Int. Ed.* **2005**, *44*, 6448–6451; c) D. L. Caulder, K. N. Raymond, *Acc. Chem. Res.* **1999**, *32*, 975–982; d) M. W. Hosseini, *Acc. Chem. Res.* **2005**, *38*, 313–323; e) C. Piguet, G. Bernardinelli, G. Hopfgartner, *Chem. Rev.* **1997**, *97*, 2005–2062; f) M. Albrecht, *Chem. Rev.* **2001**, *101*, 3457–3497.

[3] Selected examples for the assembly of small-component molecules into helices, see: a) L. Carlucci, G. Ciani, D. W. v. Gudenberg, D. M. Proserpio, *Inorg. Chem.* **1997**, *36*, 3812–3813; b) K. Biradha, C. Seward, M. J. Zaworotko, *Angew. Chem.* **1999**, *111*, 584–587; *Angew. Chem. Int. Ed.* **1999**, *38*, 492–495; c) S. R. Halper, S. M. Cohen, *Angew. Chem.* **2004**, *116*, 2439–2442; *Angew. Chem. Int. Ed.* **2004**, *43*, 2385–2388; d) F. Zhang, T. Yajima, Y.-Z. Li, G.-Z. Xu, H.-L. Chen, Q.-T. Liu, O. Yamauchi, *Angew. Chem.* **2005**, *117*, 3468–3473; *Angew. Chem. Int. Ed.* **2005**, *44*, 3402–3407; e) X.-J. Luan, Y.-Y. Wang, D.-S. Li, P. Liu, H.-M. Hu, Q.-Z. Shi, S.-M. Peng, *Angew. Chem.* **2005**, *117*, 3932–3935; *Angew. Chem. Int. Ed.* **2005**, *44*, 3864–3867; f) Y.-Q. Sun, J. Zhang, Y.-M. Chen, G.-Y. Yang, *Angew. Chem.* **2005**, *117*, 5964–5967; *Angew. Chem. Int. Ed.* **2005**, *44*, 5814–5817; g) J. Xu, K. N. Raymond, *Angew. Chem.* **2006**, *118*, 6630–6635; *Angew. Chem. Int. Ed.* **2006**, *45*, 6480–6485; h) C. S. Purohit, S. Verma, *J. Am. Chem. Soc.* **2007**, *129*, 3488–3489.

[4] Selected recent examples for nonracemic helices: a) A. Ikeda, H. Udzu, Z. Zhong, S. Shinkai, S. Sakamoto, K. Yamaguchi, *J. Am. Chem. Soc.* **2001**. *123*, 3872–3877; b) J. Yuan, M. Liu, *J. Am. Chem. Soc.* **2003**, *125*, 5051–5056; c) Y. Cui, S. J. Lee, W. Lin, *J. Am. Chem. Soc.* **2003**, *125*, 6014–6015; d) M. Seitz, A. Kaiser, S. Stempfhuber, M. Zabel, O. Reiser, *J. Am. Chem. Soc.* **2004**, *126*, 11426–11427; e) T. E. Wood, N. D. Dalgleish, E. D. Power, A. Thompson, X. Chen, Y. Okamoto, *J. Am. Chem. Soc.* **2005**, *127*, 5740–5741; f) M. Seitz, S. Stempfhuber, M. Zabel, M. Schütz, O. Reiser, *Angew. Chem.* **2005**, *117*, 246–249; *Angew. Chem. Int. Ed.* **2005**, *44*, 242–245; g) E. V. Anokhina, Y. B. Go, Y. Lee, T. Vogt, A. J. Jacobson, *J. Am. Chem. Soc.* **2006**, *128*, 9957–9962; h) H.-Y. An, E.-B. Wang, D.-R. Xiao, Y.-G. Li, Z.-M. Su, L. Xu, *Angew. Chem.* **2006**, *118*, 918–922; *Angew. Chem. Int. Ed.* **2006**, *45*, 904–908; i) K. S. Jeong, Y. S. Kim, Y. J. Kim, E. Lee, J. H. Yoon, W. H. Park, Y. W. Park, S.-J. Jeon, Z. H. Kim, J. Kim, N. Jeong, *Angew. Chem.* **2006**, *118*, 8314–8318; *Angew. Chem. Int. Ed.* **2006**, *45*, 8134–8138; j) J. Gregoliński, J. Lisowski, *Angew. Chem.* **2006**, *118*, 6268–6272; *Angew. Chem. Int. Ed.* **2006**, *45*, 6122–6126; k) J. Heo, Y.-M. Jeon, C. A. Mirkin, *J. Am. Chem. Soc.* **2007**, *129*, 7712–7713; l) K. Toyofuku, M. A. Alam, A. Tsuda, N. Fujita, S. Sakamoto, K. Yamaguchi, T. Aida, *Angew. Chem.* **2007**, *119*, 6596–6600; *Angew. Chem. Int. Ed.* **2007**, *46*, 6476–6480; m) U. Kiehne, A. Lu1tzen, *Org. Lett*, **2007**, *9*, 5333–5336.

[5] Selected recent examples for selective ionophores, see: a) Z. Grote, M.-L. Lehaire, R. Scopelliti, K. Severin, *J. Am. Chem. Soc.* **2003**, *125*, 13638–13639; b) A. Caballero, V. Lloveras, A. Tárraga, A. Espinosa, M. D. Velasco, J. Vidal-Gancedo, C. Rovira, K. Wurst, P. Molina, J. Veciana, *Angew. Chem.* **2005**, *117*, 2013–2017; *Angew. Chem. Int. Ed.* **2005**, *44*, 1977–1981; c) P. Bühlmann, E. Pretsch, E. Bakker, *Chem. Rev.* **1998**, *98*, 1593–1687.

[6] Selected recent examples for memory, see: a) A. J. Terpin, M. Ziegler, D. W. Johnson, K. N. Raymond, *Angew. Chem.* **2001**, *113*, 161–164; *Angew. Chem. Int. Ed.* **2001**, *40*, 157–160; b) R. Lauceri, A. Raudino, L. M. Scolaro, N. Micali, R. Purrello, *J. Am. Chem. Soc.* **2002**, *124*, 894–895; c) M. Ziegler, A. V. Davis, D. W. Johnson, K. N. Raymond, *Angew. Chem.* **2003**, *115*, 689–692; *Angew. Chem. Int. Ed.* **2003**, *42*, 665–668; d) G. A. Hembury, V. V. Borovkov, Y. Inoue, *Chem. Rev.* **2008**, *108*, 1–73.

[7] Selected examples for chiral amplification, see: a) M. Takeuchi, T. Imada, S. Shinkai, *Angew. Chem.* **1998**, *110*, 2242–2246; *Angew. Chem. Int. Ed.* **1998**, *37*, 2096–2099; b) X. Shi, J. C. Fettinger, J. T. Davis, *J. Am. Chem. Soc.* **2001**, *123*, 6738–6739; c) J.-L. Hou, H.-P. Yi, X.-B. Shao, C. Li, Z.-Q. Wu, X.-K. Jiang, L.-Z. Wu, C.-H. Tung, Z.-T. Li, *Angew. Chem.* **2006**, *118*, 810–814; *Angew. Chem. Int. Ed.* **2006**, *45*, 796–800.

[8] Selected examples for molecular capsulation, see: a) N. Takeda, K. Umemoto, K. Yamaguchi, M. Fujita, *Nature Nature.* **1999**, *398*, 794–796; b) F. Hof, S. L. Craig, C. Nuckolls, Jr., J. Rebek, *Angew. Chem.* **2002**, *114*, 1556–1578; *Angew. Chem. Int. Ed.* **2002**, *41*, 1488–1508; c) A. Lützen, *Angew. Chem.* **2005**, *117*, 1022–1025; *Angew. Chem. Int. Ed.* **2005**, *44*, 1000–1002; d) R. M. McKinlay, P. K. Thallapally, G. W. V. Cave, J. L. Atwood, *Angew. Chem.* **2005**, *117*, 5879–5882; *Angew. Chem. Int. Ed.* **2005**, *44*, 5733–5736; e) A. Müller, L. Toma, H. Bögge, C. Schäffer, A. Stammler, *Angew. Chem.* **2005**, *117*, 7935–7939; *Angew. Chem. Int. Ed.* **2005**, *44*, 7757–7761; f) S. Hiraoka, K. Harano, M. Shiro, M. Shionoya, *Angew. Chem.* **2005**, *117*, 2787–2791; *Angew. Chem. Int. Ed.* **2005**, *44*, 2727–2731; g) S. Hiraoka, K. Harano, M. Shiro, Y. Ozawa, N. Yasuda, K. Toriumi, M. Shionoya, *Angew. Chem.* **2006**, *118*, 6638–6641; *Angew. Chem. Int. Ed.* **2006**, *45*, 6488–6491; h) K. Harano, S. Hiraoka, M. Shionoya, *J. Am. Chem. Soc.* **2007**, *129*, 53 00–5301; i) M. Takeuchi, M. Ikeda, A. Sugasaki, S. Shinkai, *Acc. Chem. Res.* **2001**, *34*, 865–873.

[9] a) S. Hiraoka, T. Yi, M. Shiro, M. Shionoya, *J. Am. Chem. Soc.* **2002**, *124*, 14510–14511; b) S. Hiraoka, K. Harano, T. Tanaka, M. Shiro, M. Shionoya, *Angew. Chem.* **2003**, *115*, 5340–5343; *Angew. Chem. Int. Ed.* **2003**, *42*, 5182–5185; c) K. Kumazawa, Y. Yamanoi, M. Yoshizawa, T. Kusukawa, M. Fujita, *Angew. Chem.* **2004**, *116*, 6062–6066; *Angew. Chem. Int. Ed.* **2004**, *43*, 5936–5940; d) M. Yoshizawa, J. Nakagawa, K. Kumazawa, M. Nagao, M. Kawano, T. Ozeki, M. Fujita, *Angew. Chem.* **2005**, *117*, 1844–1847; *Angew. Chem. Int. Ed.* **2005**, *44*, 1810–1813; e) K. Kumazawa, K. Biradha, T. Kusukawa, T. Okano, M. Fujita, *Angew. Chem.* **2003**, *115*, 4039–4043; *Angew. Chem. Int. Ed.* **2003**, *42*, 3909–3913; f) S. Hiraoka, M. Shiro, M. Shionoya, *J. Am. Chem. Soc.* **2004**, *126*, 1214–1218; g) M. Yoshizawa, K. Ono, K. Kumazawa, T. Kato, M. Fujita, *J. Am. Chem. Soc.* **2005**, *127*, 10800–10801; h) S. Hiraoka, T. Tanaka, M. Shionoya, *J.*

Am. Chem. Soc. **2006**, *128*, 13038–13039; i) S. Hiraoka, K. Harano, M. Shionoya, *Angew. Chem.* **2004**, *116*, 3902–3906; *Angew. Chem. Int. Ed.* **2004**, *43*, 3814–3818; j) S. Leininger, B. Olenyuk, P. J. Stang, *Chem. Rev.* **2000**, *100*, 853–908.

[10] a) J. Fan, W.-Y. Sun, T. Okamura, W.-X. Tang, N. Ueyama, *Inorg. Chem.* **2003**, *42*, 3168–3175; b) J. Fan, L. Gan, H. Kawaguchi, W.-Y. Sun, K.-B. Yu, W.-X. Tang, *Chem. Eur. J.* **2003**, *9*, 3965–3973.

[11] a) S. R. Seidel, P. J. Stang, *Acc. Chem. Res.* **2002**, *35*, 972–983; b) B. Chatterjee, J. C. Noveron, M. J. E. Resendiz, J. Liu, T. Yamamoto, D. Parker, M. Cinke, C. V. Nguyen, A. M. Arif, P. J. Stang, *J. Am. Chem. Soc.* **2004**, *126*, 10645–10656; c) H.-B. Yang, K. Ghosh, A. M. Arif, P. J. Stang, *J. Org. Chem.* **2006**, *71*, 9464–9469.

[12] Selected examples, see: a) F. Rondu, G. Le Bihan, X. Wang, A. Lamouri, E. Touboul, G. Dive, T. Bellahsene, B. Pfeiffer, P. Renard, B. Guardiola-Lemaítre, D. Manéchez, L. Pénicaud, A. Ktorza, J.-J. Godfroid, *J. Med. Chem.* **1997**, *40*, 3793–3803; b) I. Ohtani, R. E. Moore, M. T. C. Runnegar, *J. Am. Chem. Soc.* **1992**, *114*, 7941–7942; c) A. Lansiaux, L. Dassonneville, M. Facompre, A. Kumar, C. E. Stephens, M. Bajic, F. Tanious, W. D. Wilson, D. W. Boykin, C. Bailly, *J. Med. Chem.* **2002**. *45*, 1994–2002; d) C. A. Parker, N. J. Anderson, E. S. J. Robinson, R. Price, R. J. Tyacke, S. M. Husbands, M. P. Dillon, R. M. Eglen, A. L. Hudson, D. J. Nutt, M. P. Crump, J. Crosby, *Biochemistry* **2004**. *43*, 16385–16392; e) I. O. Donkor, T. L. Huang, B. Tao, D. Rattendi, S. Lane, M. Vargas, B. Goldberg, C. Bacchi, *J. Med. Chem.* **2003**. *46*, 1041–1048; f) F. Rodríguez, I. Rozas, M. Kaiser, R. Brun, B. Nguyen, W. D. Wilson, R. N. García, C. Dardonville, *J. Med. Chem.* **2008**. *51*, 909–923; g) R. N. Loeppky, J. Shi, C. L. Barnes, S. Geddam, *Chem. Res. Toxicol.* **2008**. *21*, 295–307.

[13] a) N. A. Boland, M. Casey, S. J. Hynes, J. W. Matthews, M. P. Smyth, *J. Org. Chem.* **2002**, *67*, 3919–3922; b) K. Ma, J. You, *Chem. Eur. J.* **2007**, *13*, 1863–1871.

[14] a) C. Benelli, A. Dei, D. Gatteschi, *Inorg. Chem.* **1982**, *21*, 1284–1286; b) A. Dei, D. Gatteschi, E. Piergentili, *Inorg. Chem.* **1979**, *18*, 89–93; c) C. Owens, R. S. Drago, I. Bertini, C. Luchinat, L. Banci, *J. Am. Chem. Soc.* **1986**, *108*, 3298–3303.

[15] The crystal structure of $CdCl_2 \cdot 2DMF$ has been reported. The complex is a coordination polymer containing six-coordinate Cd atoms with the DMF molecules in *cis*-position, and coordination of DMF occurs through the CO−O atoms: G. Linti, H. Noeth, M. Thomann, *Z. Naturforsch. B: Chemical Sciences* **1990**, *45*, 1463–1471.

[16] CCDC-690671 ((*S,S,S*)-**4**), CCDC-690672 ((*M*)-**8**), CCDC-690673 ((*M*)-**9**), CCDC-690674 ((*M*)-**10**), and CCDC-690675 ((*P*)-**10**) contain the supplementary crystallographic data for this paper. These data can be obtained free of charge from The Cambridge Crystallographic Data Centre via www.ccdc.cam.ac.uk/data_request/cif

[17] H. D. Flack, *Acta Crystallogr. Sect. A* **1983**, *39*, 876–881.

[18] H.-T. Chang, C.-T. Chen, T. Kondo, G. Siuzdak, K. B. Sharpless, *Angew. Chem.* **1996**, *108*, 202–206; *Angew. Chem. Int. Ed. Engl.* **1996**, *35*, 182–186.

Received: June 12, 2008
Revised: September 4, 2008